Measurement of Linear Response Functions in NMR

Tao Xin,[1,2] Julen S. Pedernales,[3] Lucas Lamata,[3] Enrique Solano,[3,4] and Gui-Lu Long[1,2,5,*]

[1]*State Key Laboratory of Low-dimensional Quantum Physics and Department of Physics, Tsinghua University, Beijing 100084, China*
[2]*Tsinghua National Laboratory of Information Science and Technology, Beijing 100084, China*
[3]*Department of Physical Chemistry, University of the Basque Country UPV/EHU, Apartado 644, 48080 Bilbao, Spain*
[4]*IKERBASQUE, Basque Foundation for Science, Maria Diaz de Haro 3, 48013 Bilbao, Spain*
[5]*The Innovative Center of Quantum Matter, Beijing 100084, China*

(Dated: June 3, 2016)

We measure multi-time correlation functions of a set of Pauli operators on a two-level system, which can be used to retrieve its associated linear response functions. The two-level system is an effective spin constructed from the nuclear spins of ^{1}H atoms in a solution of ^{13}C-labeled chloroform. Response functions characterize the linear response of the system to a family of perturbations, allowing us to compute physical quantities such as the magnetic susceptibility of the effective spin. We use techniques exported from quantum information to measure time correlations on the two-level system. This approach requires the use of an ancillary qubit encoded in the nuclear spins of the ^{13}C atoms and a sequence of controlled operations. Moreover, we demonstrate the ability of such a quantum platform to compute time-correlation functions of arbitrary order, which relate to higher-order corrections of perturbative methods. Particularly, we show three-time correlation functions for arbitrary times, and we also measure time correlation functions at fixed times up to tenth order.

arXiv:1606.00686v1 [quant-ph] 2 Jun 2016

Introduction—In nature, closed quantum systems exist only as a convenient approximation. When systems are subjected to perturbations or have strong interactions with their environment, open models yield a more reliable description. A complete statistical characterization of an open quantum system unavoidably involves knowledge on the expectation value of multi-time correlations of observables, which are related to measurable quantities [1]. Time-correlation functions are at the core of optical coherence theory [2], and can also be used for the quantum simulation of Lindbladian dynamics [3]. A plethora of physical magnitudes, such as susceptibilities and transport coefficients, can be microscopically derived in terms of time correlation functions [4, 5]. In a statistical approach [4], linear response functions represent a powerful tool to compute the susceptibility of an observable to a perturbation on the system. Such a function is constructed in terms of time-correlation functions of unperturbed observables.

Despite the ubiquity of time correlations in physics, their measurement on a quantum mechanical system is not straightforward. This difficulty lies in the fact that in quantum mechanics the measurement process disturbs the system, leaving it unreliable for a later correlated observation. Statistical descriptions typically involve an averaging of the time-correlation functions over an ensemble of particles. In such a case, it is possible to measure operator A at time t_1 over a reduced number of particles of the ensemble, and operator B at time t_2 over particles that were not perturbed by the first measurement. However, it is not always possible to perform measurements discriminating a subset of particles out of an ensemble. Moreover, nowadays, single quantum systems offer a high degree of controllability, which legitimates the interest in measuring time-correlation functions on single quantum systems. A solution to this puzzle can be found in algorithms for quantum computation. It is known that introducing an ancillary two-level system and performing a reduced set of controlled operations, time-correlation functions of a system can be reconstructed from single-time observables of the ancilla [6–8]. In this Letter, we measure n-time correlation functions for pure states, up to $n = 10$, in a highly-controllable quantum platform as is the case of nuclear magnetic resonance (NMR). Moreover, we frame these correlation functions in the context of linear response theory to compute physical magnitudes including the susceptibility of the system to perturbations. Finally, the scalability of the approach is shown to be efficient for multi-time correlation functions.

The algorithm—We will follow the algorithm introduced in Ref. [7] to extract n-time correlation functions of the form $f(t_1, ..., t_{n-1}) = \langle\phi|\sigma_\gamma(t_{n-1})...\sigma_\beta(t_1)\sigma_\alpha(0)|\phi\rangle$ from a two-level quantum system, with the assistance of one ancillary qubit. Here, $|\phi\rangle$ is the quantum state of the system and $\sigma_\alpha(t)$ is a time-dependent Pauli operator in the Heisenberg picture, defined as $\sigma_\alpha(t) = U^\dagger(t;0)\sigma_\alpha U(t;0)$, where $\alpha = x, y, z$, and $U(t_j;t_i)$ is the evolution operator from time t_i to t_j. The considered algorithm of Ref. [7] is depicted in Fig. (1), for the case where qubit A and B respectively encode the ancillary qubit and the two-level quantum system, and consists of the following steps:
(i) The input state of the probe-system qubits is prepared in $\rho_{\rm in}^{\rm AB} = |+\rangle\langle+| \otimes \rho_{\rm in}$, with $|+\rangle = (|0\rangle + |1\rangle)/\sqrt{2}$ and $\rho_{\rm in} = |\phi\rangle\langle\phi|$.
(ii) The controlled quantum gate $U_\alpha^k = |1\rangle\langle1| \otimes S_\alpha + |0\rangle\langle0| \otimes \mathbb{I}_2$ is firstly applied on the two qubits, with $S_x = \sigma_x$, $S_y = -i\sigma_y$ and $S_z = i\sigma_z$. $\mathbb{I}_2$ is a 2×2 identity matrix.
(iii) It follows a unitary evolution of the system qubit from t_k to time t_{k+1}, $U(t_{k+1};t_k)$, which needs not be known to the experimenter. In our setup, we engineer this dynamics by decoupling qubit A and B, such that only the system qubit evolves under its free-energy Hamiltonian. An additional evolution can also be imposed on the system qubit according to the considered problem. Steps (ii) and (iii) will be iterated n times, taking k from 0 to $n-1$ and avoiding step (iii) in the last iteration. With this, all n Pauli operators will

be interspersed between evolution operators with the time intervals of interest $\{t_k, t_{k+1}\}$.
(iv) Finally, the time correlation function is extracted as a non-diagonal operator of the ancilla, $\mathrm{Tr}(|0\rangle\langle 1|\varphi_{\mathrm{out}}\rangle\langle\varphi_{\mathrm{out}}|)$, where $|\varphi_{\mathrm{out}}\rangle = (|0\rangle \otimes U(t_{n-1};0)|\phi\rangle + |1\rangle \otimes S_\gamma U(t_{n-1};t_{n-2})...U(t_2;t_1)S_\beta U(t_1;0)S_\alpha|\phi\rangle)/\sqrt{2}$. We recall here that $|0\rangle\langle 1| = (\sigma_x + i\sigma_y)/2$, such that $f(t_1,...,t_{n-1}) = c_y c_z(\langle\sigma_x\rangle + i\langle\sigma_y\rangle)$, which is in general a complex magnitude. The additional factors $c_y = i^r$ and $c_z = (-i)^l$, where integers r and l are the occurrence numbers of Pauli operators σ_y and σ_z in $f(t_1,...,t_{n-1})$.

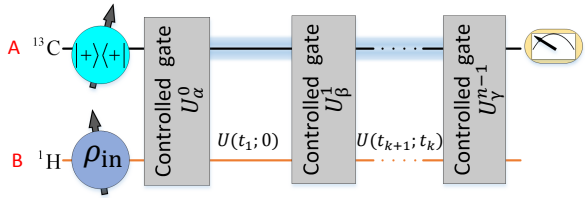

Figure 1. **Two-qubit quantum circuit for measuring general n-time correlation functions.** Qubit A is the ancilla (held by the nuclear spin of ^{13}C), and qubit B is the system qubit (held by the nuclear spin of ^{1}H). The blue zone between the different controlled gates U_α^k on the line of qubit A represents the decoupling of the ^{13}C nucleus from the nuclear spin of ^{1}H, while the latter evolves according to $U(t_{k+1};t_k)$. The measurement of the quantities $\langle\sigma_x\rangle$ and $\langle\sigma_y\rangle$ of the ancillary qubit at the end of the circuit will directly provide the real and imaginary values of the n-time correlation function for the initial state $\rho_{\mathrm{in}} = |\phi\rangle\langle\phi|$.

The measurement of n-time correlation functions plays a significant role in the linear response theory. For instance, we can microscopically derive useful quantities such as the conductivity and the susceptibility of a system, with the knowledge of 2-time correlation functions. As an illustrative example, we study the case of a spin-1/2 particle in a uniform magnetic field of strength B along the z-axis, which has a natural Hamiltonian $\mathcal{H}_0 = -\gamma B\sigma_z$, where γ is the gyromagnetic ratio of the particle. We assume now that a magnetic field with a sinusoidal time dependence $B_0' e^{-i\omega t}$ and arbitrary direction α perturbs the system. The Hamiltonian representation of such a situation is given by $\mathcal{H} = \mathcal{H}_0 - \gamma B_0'\sigma_\alpha e^{-i\omega t}$, with $\alpha = x, y, z$. The deviation of the expectation value of the magnetic moment $\mu_\beta = \gamma\sigma_\beta$ in direction $\beta = x, y, z$, in presence of the perturbation, from its unperturbed value, is called the susceptibility of the magnetic moment for a perturbation in direction α. It is given by $\mu_\beta(t) = \mu_\beta(0) + \chi^\omega_{\alpha,\beta} e^{-i\omega t}$, where $\chi^\omega_{\alpha,\beta}$ is the frequency-dependent susceptibility. From linear response theory, we learn that the susceptibility can be retrieved integrating the linear response function as $\chi^\omega_{\alpha,\beta} = \int_{-\infty}^{t} \phi_{\alpha,\beta}(t-s)e^{-i\omega(t-s)}ds$. Moreover, the latter can be given in terms of time-correlation functions of the measured and perturbed observables, $\phi_{\alpha,\beta}(t) = \langle[\gamma B\sigma_\alpha, \gamma\sigma_\beta(t)]\rangle/(i\hbar)$, where $\sigma_\beta(t) = e^{i/\hbar H_0 t}\sigma_\beta e^{-i/\hbar H_0 t}$. So far, the response function can be retrieved by measuring the 2-time correlation functions of the unperturbed system $\langle\sigma_\alpha\sigma_\beta(t)\rangle$ and $\langle\sigma_\beta(t)\sigma_\alpha\rangle$. Notice that when $\alpha = \beta$, $\langle\sigma_\alpha(t)\sigma_\alpha\rangle^* = \langle\sigma_\alpha\sigma_\alpha(t)\rangle$, and it is enough to measure one of them.

The experiment—We will measure n-time correlation functions of a two-level quantum system with the assistance of one ancillary qubit by implementing the quantum circuit shown in Fig. (1). Experiments are carried out using NMR [9–11], where the sample used is ^{13}C-labeled chloroform. Nuclear spins of ^{13}C and ^{1}H encode the ancillary qubit and the two-level quantum system, respectively. With the weak coupling approximation, the internal Hamiltonian of ^{13}C-labeled chloroform is

$$\mathcal{H}_{\mathrm{int}} = -\pi(\nu_1-\omega_1)\sigma_z^1 - \pi(\nu_2-\omega_2)\sigma_z^2 + 0.5\pi J_{12}\sigma_z^1\sigma_z^2, \quad (1)$$

where ν_j $(j = 1, 2)$ is the chemical shift, J_{12} is the J-coupling strength as illustrated in Ref. [12], while ω_1 and ω_2 are reference frequencies of ^{13}C and ^{1}H, respectively. We set $\nu_1 = \omega_1$ and $\nu_2 - \omega_2 = \triangle\omega$ such that the natural Hamiltonian of the system qubit is $\mathcal{H}_0 = -\pi\triangle\omega\sigma_z$. The detuning frequency $\triangle\omega$ is chosen as hundreds of Hz to assure the selective excitation of different nuclei via hard pulses. All experiments are carried out on a Bruker AVANCE 400MHz spectrometer at room temperature.

It is widely known that the thermal equilibrium state of an NMR ensemble is a highly-mixed state with the following structure [9]

$$\rho_{eq} \approx \frac{1-\epsilon}{4}\mathbb{I}_4 + \epsilon(\frac{1}{4}\mathbb{I}_4 + \sigma_z^1 + 4\sigma_z^2). \quad (2)$$

Here, $\mathbb{I}_4$ is a 4×4 identity matrix and $\epsilon \approx 10^{-5}$ is the polarization at room temperature. Given that $\mathbb{I}_4$ remains unchanged and that it does not contribute to the NMR spectra, we consider the deviation density matrix $\triangle\rho = 0.25\mathbb{I}_4 + \sigma_z^1 + 4\sigma_z^2$ as the effective density matrix describing the system. The deviation density matrix can be initialized in the pure state $|00\rangle\langle 00|$ by the spatial averaging technique [13–15], transforming the system into a so-called pseudo-pure state (PPS). Input state $\rho_{\mathrm{in}}^{\mathrm{CH}}$ can be easily created by applying local single-qubit rotation pulses after the preparation of the PPS.

In Step (ii), all controlled quantum gates U_α^k can be easily realized by using single-qubit rotation pulses and a J-coupling evolution [16, 17]. All controlled operations are chosen from the set of gates $\{C - R_z^2(-\pi), C - iR_x^2(\pi), C - R_y^2(\pi)\}$. The notation $C - U$ means operator U will be applied on the system qubit only if the ancilla qubit is in state $|1\rangle\langle 1|$, while $R_{\hat{n}}^j(\theta)$ represents a single-qubit rotation on qubit j along the $\hat{n}$-axis with the rotation angle θ. In an NMR platform, we decompose gates U_α^k in the following way,

$$\begin{aligned}
C - R_z^2(-\pi) &= U(\frac{1}{2J})R_z^2(-\frac{\pi}{2}),\\
C - iR_x^2(\pi) &= \sqrt{i}R_z^1(\frac{\pi}{2})R_z^2(-\frac{\pi}{2})R_x^2(\frac{\pi}{2})U(\frac{1}{2J})R_y^2(\frac{\pi}{2}),\\
C - R_y^2(\pi) &= R_x^2(\frac{\pi}{2})U(\frac{1}{2J})R_x^2(-\frac{\pi}{2})R_y^2(\frac{\pi}{2}). \quad (3)
\end{aligned}$$

Here, $U(\frac{1}{2J})$ is the J-coupling evolution $e^{-i\pi\sigma_z^1\sigma_z^2/4}$. Moreover, any z-rotation $R_z(\theta)$ can be decomposed in

terms of rotations around the x and y axes, $R_z(\theta) = R_y(\pi/2)R_x(-\theta)R_y(-\pi/2)$. On the other hand, the decoupling of the interaction between ^{13}C and ^{1}H nuclei can be realized by using refocusing pulses [18] or the Waltz-4 sequence [19–21].

We will now apply the described algorithm to a collection of situations of physical interest. The detailed NMR sequences for all considered experiments can be found in Ref. [12]. In Fig. (2), we extract the time-correlation functions of a two-level system evolving under Hamiltonian $\mathcal{H}_0 = -100\pi\sigma_z$ for a collection of α and β, and different initial states. These correlation functions are enough to retrieve the response function for a number of physical situations corresponding to different magnetic moments and applied fields. In this experiment, $\mathcal{H}_0$ is realized by setting $\nu_1 = \omega_1$ and $\nu_2 - \omega_2 = 100$ Hz in Eq. (1). A rotation pulse $R_y^1(\pi/2)$ is applied on the first qubit after the PPS preparation to create $\rho_{\rm in}^{\rm CH} = |+\rangle\langle+| \otimes |0\rangle\langle 0|$. Similarly, a π rotation on the second qubit is additionally needed to prepare $\rho_{\rm in}^{\rm CH} = |+\rangle\langle+|\otimes|1\rangle\langle 1|$ as the input state of the ancilla-system compound, or alternatively a $R_y^2(\pi/2)$ rotation to generate the initial state $\rho_{\rm in}^{\rm CH} = |+\rangle\langle+| \otimes |+\rangle\langle+|$.

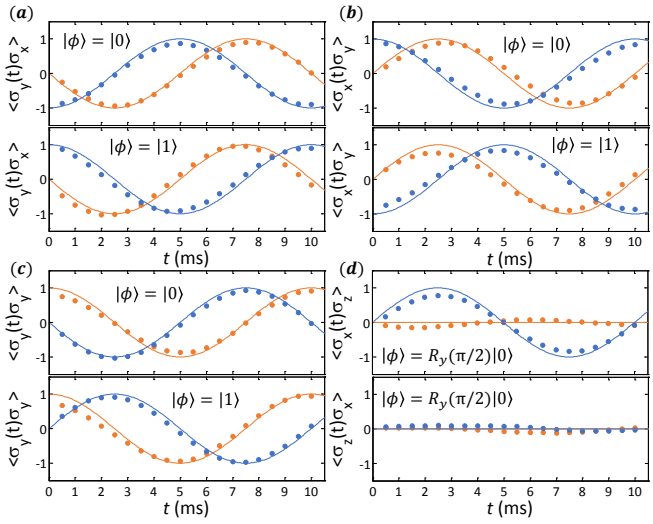

Figure 2. **Experimental results (dots) for 2-time correlation functions.** In this case, only two controlled quantum gates U_α^0 and U_β^1 are applied with an interval of t. For example, U_α^0 and U_β^1 should be chosen as $C - iR_x^2(\pi)$ and $C - R_y^2(\pi)$, respectively, to measure the 2-time correlation function $\langle\sigma_y(t)\sigma_x\rangle$. t is swept from 0.5ms to 10ms with a 0.5ms increment. The input state of ^{1}H nuclei $\rho_{\rm in} = |\phi\rangle\langle\phi|$ is shown on each diagram. All experimental results are directly obtained from measurements of the expectation values of $\langle\sigma_x\rangle$ and $\langle\sigma_y\rangle$ of the ancillary qubit.

We now consider a more involved situation where the system is in a magnetic field with an intensity that is decaying exponentially in time, that is, the unperturbed system Hamiltonian turns now into a time-dependent $\mathcal{H}' = \gamma B_0 e^{-at}\sigma_y$. In this case, the response function needs to be computed in terms of time-correlation functions of the system observables evolving under this new Hamiltonian. In Fig. (3), we show such a case, for the time-correlation function $\langle\sigma_x(t)\sigma_x\rangle$ and the initial state $(|0\rangle - i|1\rangle)/\sqrt{2}$. For this, we set $\nu_1 = \omega_1$ and $\nu_2 = \omega_2$ in Eq. (1), making the system free Hamiltonian $\mathcal{H}_0 = 0$. The initial state $|\phi\rangle = R_x(\pi/2)|0\rangle$ can be prepared by using a rotation pulse $R_x(\pi/2)$ on the initial PPS. Two controlled quantum gates $U_x^0 = C - iR_x^2(\pi)$ and $U_x^1 = C - iR_x^2(\pi)$ are applied with a time interval t. A decoupling sequence Waltz-4 [19] is used to cancel the interaction between the ^{13}C and ^{1}H nuclei during the evolution between the controlled operations. During the decoupling period, a time-dependent radio-frequency pulse is applied on the resonance of the system qubit ^{1}H to create the Hamiltonian $\mathcal{H}'(t) = 500e^{-300t}\pi\sigma_y$.

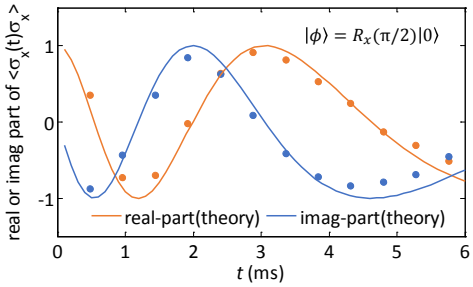

Figure 3. **Experimental results (dots) for a 2-time correlation function of the ^{1}H nuclei evolving under a time-dependent Hamiltonian.** For this experiment, the ^{1}H nuclei have a natural Hamiltonian $\mathcal{H}_0 = 0$ and an initial state $|\phi\rangle = R_x(\pi/2)|0\rangle$. An evolution $U(t;0)$ between U_x^0 and U_x^1 is applied on the system, which is described by the evolution operator $e^{-i\int_0^t \mathcal{H}'(s)ds}$ with $\mathcal{H}'(s) = 500e^{-300s}\pi\sigma_y$. t is changed from 0.48ms to 5.76ms with a 0.48ms increment per step.

We now move to explore higher-order correlation functions, which are related to higher-order corrections in perturbation theory. In Fig. (4), we show real and imaginary parts of 3-time correlation functions as compared to their theoretically expected values. We measure the 3-time correlation function $\langle\sigma_y(t_2)\sigma_y(t_1)\sigma_z\rangle$ versus t_1 and t_2. In this case, we simulate the system-qubit free Hamiltonian $\mathcal{H}_0 = -200\pi\sigma_z$ and an input state $\rho_{\rm in} = |0\rangle\langle 0|$. For this, we set $\nu_1 = \omega_1$ and $\nu_2 - \omega_2 = 200$ Hz in Eq. (1). The J-coupling term of Eq. (1) will be canceled by using a refocusing pulse in the circuit. Three controlled quantum gates U_α^0, U_β^1 and U_γ^2 should be chosen as $C - R_z^2(-\pi)$, $C - R_y^2(\pi)$ and $C - R_y^2(\pi)$. The free evolution of the ^{1}H nuclei between U_α^0 and U_β^1 is given by the evolution operator $e^{-i\mathcal{H}_0 t_1}$. Accordingly, the free evolution of the ^{1}H nuclei between U_β^1 and U_γ^2 is given by $e^{-i\mathcal{H}_0(t_2-t_1)}$. However, when t_2<t_1, we perform the evolution $e^{-i(-\mathcal{H}_0)(t_1-t_2)}$ by inverting the phase of the Hamiltonian $\mathcal{H}_0$, which is realized by using double π pulses at the beginning and at the end of the evolution [16]. The data shown in Fig. (4) demonstrates the power of this algorithm, with full range 3-time correlation functions, for all combinations of t_1 and t_2.

For testing scalability, we also measure higher-order time-correlation functions, up to $n = 10$. In this case, we con-

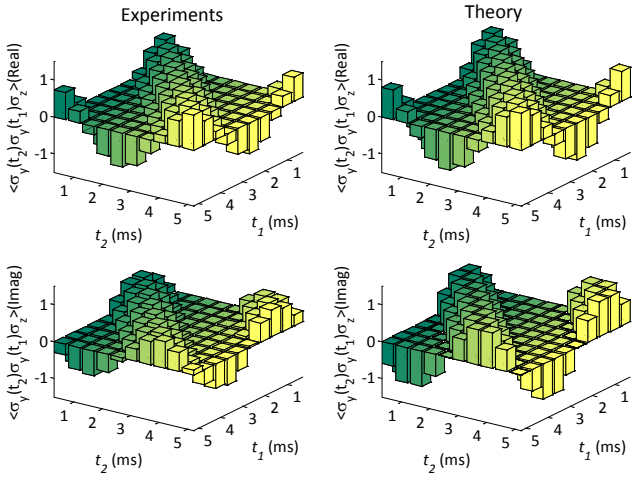

Figure 4. **Experimental results for the 3-time correlation functions.** We plot $\mathcal{M}^3_{zyy} = \langle\sigma_y(t_2)\sigma_y(t_1)\sigma_z\rangle$ for t_1 and t_2 going from 0.5ms to 5ms with 0.5ms time step, showing the agreement of experimental results with theoretical predictions. The quantum circuit for measuring $\mathcal{M}^3_{zyy}$ includes three controlled quantum gates U^0_z, U^1_y and U^2_y, which are decomposed according to Eq. (3) and experimentally implemented by hard pulses.

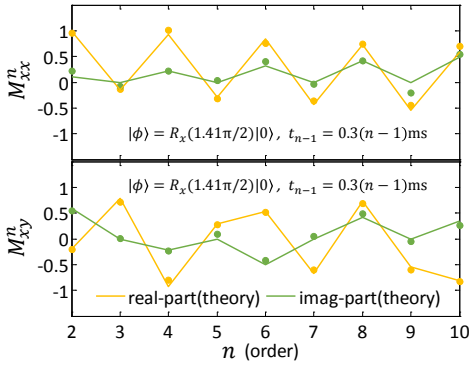

Figure 5. **Experimental results (dots) for high-order time-correlation functions $\mathcal{M}^n_{xx}$ and $\mathcal{M}^n_{xy}$ ($n = 2, 3, ..., 10$).** n controlled quantum gates U^0_α,U^1_β,...,U^{n-1}_γ are sequentially applied with a time interval $\triangle t = 0.3$ms. Refocusing pulses are used to decouple the interaction between the nuclei of ^{13}C and ^{1}H, during the time intervals $\triangle t$ between gates. For this experiment, we use the GRAPE pulsed technique to implement the quantum circuit. Using hard pulses like in the previous experiments would result in poor quality of the measured data due to the high number of pulses required and the cumulative effect of their imperfections.

sider the free Hamiltonian $\mathcal{H}_0 = -100\pi\sigma_z$ and the input state $|\phi\rangle = R_x(1.41\pi/2)|0\rangle$, and we measure the following high-order correlation functions as a function of the correlation order n, with time intervals $t_{n-1} = 0.3(n-1)$ ms,

$$\begin{aligned}\mathcal{M}^n_{xx} &= \langle\sigma_x(t_{n-1})\sigma_x(t_{n-2})...\sigma_x(t_1)\sigma_x\rangle,\\ \mathcal{M}^n_{xy} &= \langle...\sigma_x(t_{2m})\sigma_y(t_{2m-1})...\sigma_y(t_1)\sigma_x\rangle.\end{aligned} \tag{4}$$

Here, the superscripts and subscripts of $\mathcal{M}$ are the order of the correlation and the involved Pauli operators, respectively. Index m runs from 1 to $(n-1)/2$ for odd n, and to $n/2$ for even n. The quantum circuit used to measure $\mathcal{M}^n_{xx}$ and $\mathcal{M}^n_{xy}$ is based in the gradient ascent pulse engineering (GRAPE) technique [22, 23], which is designed to be robust to the static field distributions (T^*_2 process) and RF inhomogeneities. High-order correlation functions are related to the system susceptibilities beyond the linear response. In Fig. 5, we show the measured results for this case, demonstrating the scalability of the technique and the high accuracy even for a 10-time correlation function.

For all cases here discussed, experimental data shows a high degree of agreement with the theoretical predictions. Error bars are not shown, as they are always smaller than the used dots themselves. In our setup, the sources of errors are related to the initialization of the PPS, and imperfections in the width of the employed hard pulses. Moreover, the latter effect is cumulative and can result in a snowball effect. Additionally, factors such as T^*_2 processes, RF inhomogeneities, and measurement errors, bring in a signal loss.

Conclusion—We have shown that the measurement of time-correlation functions of arbitrary order in NMR is an efficient task, and can be used to obtain the linear response function of the system. We have demonstrated that such magnitudes can be experimentally retrieved with high accuracy, opening the door to the quantum simulation of physical models where time correlations play a central role. These experimental techniques are platform independent and may be extended to systems of arbitrary size, where a single ancillary qubit will always suffice.

Acknowledgments. T. X. and G.-L. L. are grateful to the following funding sources: National Natural Science Foundation of China under Grants No. 11175094 and No. 91221205; National Basic Research Program of China under Grant No. 2015CB921002. J. S. P., L. L. and E. S. acknowledge support from Spanish MINECO FIS2015-69983-P; UPV/EHU UFI 11/55; Ramón y Cajal Grant RYC-2012-11391; UPV/EHU Project EHUA14/04 and a UPV PhD grant.

* Correspondence and requests for materials should be addressed to G.L.L.: gllong@tsinghua.edu.cn

[1] H. P. Breuer and F. Petruccione, *The Theory of Open Quantum Systems* (Oxford University Press, New York 2002).
[2] R. J. Glauber, Phys. Rev. **130**, 2529 (1963).
[3] R. Di Candia, J. S. Pedernales, A. del Campo, E. Solano, J. Casanova, Sci. Rep. **5**, 9981 (2015).
[4] R. Kubo, J. Phys. Soc. Jpn. **12**, 570 (1957).
[5] R. Zwanzig, Annu. Rev. Phys. Chem. **16**, 67 (1965).
[6] R. Somma, G. Ortiz, J. E. Gubernatis, E. Knill, and R. Laflamme, Phys. Rev. A **65**, 042323 (2002).
[7] J. S. Pedernales, R. Di Candia, I. L. Egusquiza, J. Casanova, and E. Solano, Phys. Rev. Lett. **113**, 020505 (2014).
[8] A. M. Souza, I. S. Oliveira, and R. S. Sarthour, New J. of Phys. **13**, 053023 (2011).
[9] D. G. Cory, R. Laflamme, E. Knill, L. Viola, T. F. Havel, N. Boulant, G. Boutis, E. Fortunato, S. Lloyd, R. Martinez, et. al., Fortschr. Phys. **48**, 875 (2000).
[10] T. F. Havel, D. G. Cory, S. Lloyd, N. Boulant, E. M. Fortu-

nato, M. A. Pravia, G. Teklemariam, Y. S. Weinstein, A. Bhattacharyya, and J. Hou, Am. J. Phys. **70**, 345 (2002).
[11] D. Suter and T. S. Mahesh, J. Chem. Phys. **128**, 052206 (2008).
[12] See the Supplemental Material for additional details.
[13] D. G. Cory, A. F. Fahmy, and T. F. Havel, PNAS **94**, 1634 (1997).
[14] D. G. Cory, M. D. Price, and T. F. Havel, Physica D **120**, 82 (1998).
[15] E. Knill, I. Chuang, and R. Laflamme, Phys. Rev. A **57**, 3348 (1998).
[16] L. M. K. Vandersypen and I. L. Chuang, Rev. Mod. Phys. **76**, 1037 (2005).
[17] T. Xin, H. Li, B.-X. Wang, and G.-L. Long, Phys. Rev. A **92**, 022126 (2015).
[18] M. R. Bendall and R. E. Gordon, J. Magn. Reson. **53**, 365 (1983).
[19] S. Widmaier, J. Breuer, W.-I. Jung, G. J. Dietze, and O. Lutz, J. Magn. Reson. Imaging **16**, 845 (1998).
[20] A. J. Shaka, J. Keeler, and R. Freeman, J. Magn. Reson. **53**, 313 (1983).
[21] A. J. Shaka, J. Keeler, T. Frenkiel, and R. Freeman, J. Magn. Reson. **52**, 335 (1983).
[22] N. Khaneja, T. Reiss, C. Kehlet, T. Schulte-Herbrüggen, and S. J. Glaser, J. Magn. Reson. **172**, 296 (2005).
[23] C. A. Ryan, C. Negrevergne, M. Laforest, E. Knill, and R. Laflamme, Phys, Rev. A **78**, 012328 (2008).

SUPPLEMENTAL MATERIAL

DETAILS OF EXPERIMENTAL IMPLEMENTATION

Experiments are carried out using nuclear magnetic resonance (NMR), where the sample ^{13}C-labeled chloroform is used as our two-qubit quantum computing processor. ^{13}C and ^{1}H in the chloroform act as the ancillary qubit and system qubit, respectively. Fig. 6 shows the molecular structure and properties of the sample. The top plot in Fig. 7 presents some experimental spectra, such as the spectra of the thermal equilibrium and pseudo pure state. The bottom plot in Fig. 7 shows NMR spectra which is created after we measure the 2-time correlation function $\mathcal{M}_{xy}^{n}$ $(n = 2)$ in the main text.

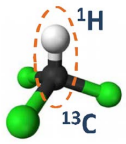

	13C	1H	T_1(s)	T_2(s)
13C	-7787.9		18.8	0.35
1H	215.09	-3206.5	10.9	3.3

Figure 6. **Molecular structure and relevant parameters of ^{13}C-labeled chloroform.** Diagonal elements and off-diagonal elements in the table provide the values of the chemical shifts (Hz) and J-coupling constant (Hz) between ^{13}C and ^{1}H nuclei of the molecule. The right table also provides the longitudinal time T_1 and transversal relaxation T_2 , which can be measured using the standard inversion recovery and Hahn echo sequences.

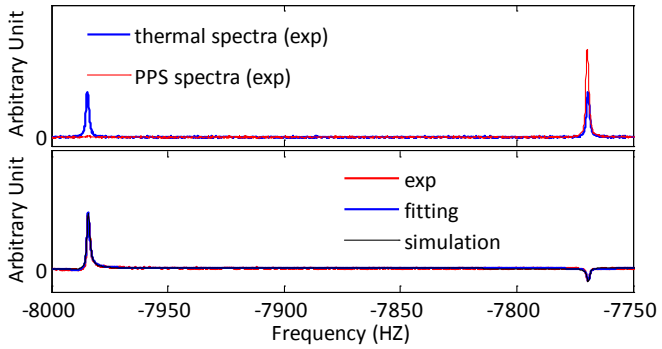

Figure 7. **Experimental spectra of ^{13}C nuclei.** The blue line of the top plot shows the observed spectrum after a $\pi/2$ pulse is applied on ^{13}C nuclei in the thermal equilibrium state. The signal measured after applying a $\pi/2$ pulse following the preparation of the PPS is shown by the red line of the top plot. The bottom plot shows the spectrum when we measure $\mathcal{M}_{xy}^{n}$ $(n = 2)$ in the main text. The red, blue and black lines represent the experimental spectra, fitting results and corresponding simulations, respectively.

The detailed NMR sequences for measuring n-time correlation functions in the three types of experiments in the main text are illustrated in Figs. 8(a), (b) and (c). As an example, Fig. 8(a) shows the experimental sequence for measuring $\langle\sigma_y(t)\sigma_x\rangle$. Other time correlation functions $\langle\sigma_x(t)\sigma_y\rangle$ and $\langle\sigma_y(t)\sigma_y\rangle$ can be measured in a similar way by replacing the corresponding controlled quantum gates. In the NMR sequence shown in Fig. 8(c), we use the decoupling sequence Waltz-4, whose basic pulses are as

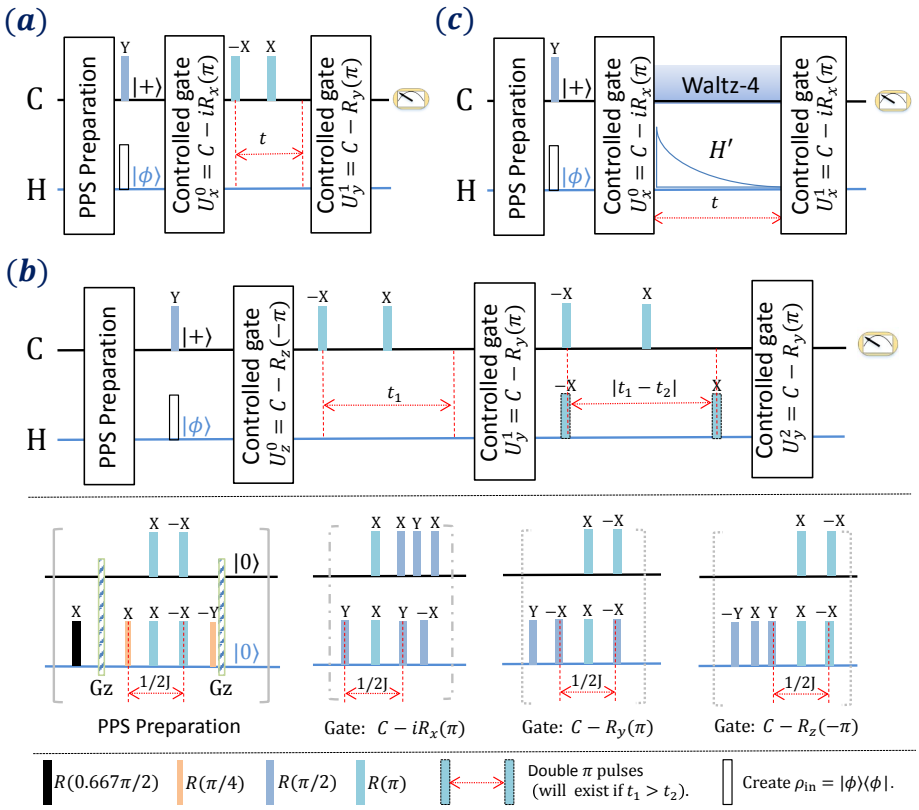

Figure 8. **NMR sequence to realize the quantum algorithm for measuring n-time correlation functions.** The black line and blue line mean the ancillary qubit (marked by ^{13}C) and the system qubit (marked by ^{1}H). All the controlled quantum gates U_α^k are decomposed into the following sequence in the bottom of the plot. Gz means a z-gradient pulse which is used to cancel the polarization in $x-y$ plane. (a) NMR sequence for measuring the 2-time correlation function $\langle\sigma_y(t)\sigma_x\rangle$. Other 2-time correlation functions can be similarly measured. (b) NMR sequence for measuring the 3-time correlation function $\langle\sigma_y(t_2)\sigma_y(t_1)\sigma_z\rangle$. We use the so-called double π pulses which will exist if t_1 is longer than t_2, to invert the phase of the Hamiltonian $\mathcal{H}_0$. (c) NMR sequence for measuring the 2-time correlation function $\langle\sigma_x(t)\sigma_x\rangle$ with a time-dependent Hamiltonian $\mathcal{H}'(t)$. The method to decouple the interaction between ^{13}C and ^{1}H nuclei is Waltz-4 sequence. Hamiltonian $\mathcal{H}'(t) = 500e^{-300t}\pi\sigma_y$ is created by using a special time-dependent radio-frequency pulse on the resonance of the second qubit in the ^{1}H nuclei.

follows,

$$[R_{-x}(\tfrac{3\pi}{2})R_x(\pi)R_{-x}(\tfrac{\pi}{2})]^2[R_x(\tfrac{3\pi}{2})R_{-x}(\pi)R_x(\tfrac{\pi}{2})]^2. \tag{5}$$

This efficiently cancels the coupling between the ^{13}C and ^{1}H nuclei such that the ^{1}H nucleus is independently governed by the external Hamiltonian $\mathcal{H}'(t)$.